Laser Absorption Characteristics of a Simulated Rotating Detonation Rocket Engine

Mathias C. Ross, Ann R. Karagozian
University of California at Los Angeles
Los Angeles, CA, USA
&
Jason R. Burr
Air Force Research Laboratory
Edwards AFB, CA, USA

1 Introduction

In order for rotating detonation rocket engine (RDRE) technology to develop, it is necessary to have a true understanding of what is happening inside the combustion chamber. However, RDRE flowfields are difficult to measure: rapid fluctuations in temperature and pressure make it challenging to design accurate temporally-resolved diagnostics. Recently, advances in laser absorption spectroscopy (LAS) has made it possible to take MHz-resolution measurements of pressure, temperature, and species composition in RDRE applications [1,2]; however, these diagnostics are currently limited to regions downstream of the detonations themselves.

In this work, a three-dimensional simulation of a gaseous methane-oxygen RDRE is presented in the context of taking LAS measurements in the detonation region. A methodology is presented for considering an idealized laser diagnostic, and several candidate species are considered for targeted measurements. Further, possible measurements are considered in the context of the information that would be useful in evaluating detonation strength, and in assessing RDRE operation.

2 Simulation Setup

2.1 Geometry

The present study was based on an annular combustion chamber, with a length and outer chamber diameter of 76.2 mm, and an inner diameter of 66.2 mm. Gaseous methane and oxygen were injected to the engine through 72 impinging fuel-ox injector pairs, each with a 60 degree impingement angle. Each of the 72 fuel injectors had a diameter of 0.787 mm, and each ox injector had a diameter of 1.245 mm; the injector pairs were evenly spaced azimuthally around the annulus.

2.2 Numerics

The simulation matched flow conditions for an experiment conducted at the Air Force Research Laboratory, and were set with reactant mass flow of $\dot{m} = 0.26$ kg/s and $\phi = 1.1$. The ALREST (Advanced

Correspondence to: rossmathiasc@ucla.edu

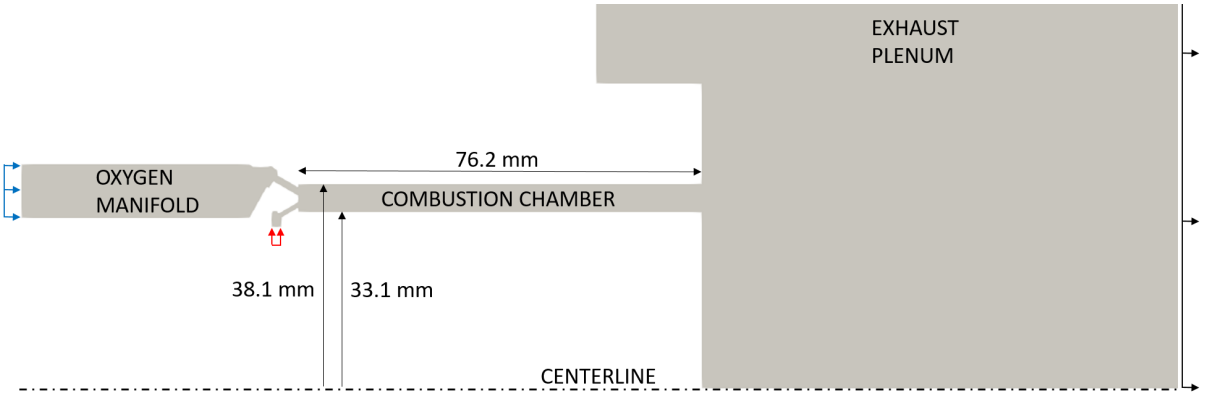

Figure 1: Cross-section of the domain used by the simulation; in the interest of space, representation of the outflow plenum is truncated.

Table 1: Boundary conditions enforced at flow inlets and outlets.

Enforced Condition	**Value**
Fuel Mass Flow Rate (kg/s)	0.06
Fuel Temperature (K)	300
Oxidizer Mass Flow Rate (kg/s)	0.20
Oxidizer Temperature (K)	300
Co-flow Velocity (m/s)	1
Co-flow Temperature (K)	300
Subsonic Outflow Pressure (Pa)	9.2×10^4

Liquid-Rocket Engine Scaling Tool) High-Fidelity Modeling framework was used to run the simulation, which is in turn based on the Large Eddy Simulation with Linear Eddy (LESLIE) code developed at the Georgia Institute of Technology [3, 4]. Reacting LES-filtered Navier–Stokes equations were simulated using a 2nd-order McCormack finite-volume scheme, with an additional turbulent closure. Additionally, a MUSCL upwinding scheme was included in order to handle discontinuities expected at detonation wave fronts. Methane-oxygen chemistry was modeled using the FFCMy-12 mechanism, which tracks 12 species and 38 reactions [5, 6].

The simulation domain extended beyond the combustion chamber: fuel/oxidizer plenums upstream of the injectors, all 72 injector pairs, and flow downstream of the engine were all included within the domain. A cross-section of the domain is shown in Fig. 1. Non-slip, adiabatic boundary conditions were enforced at the engine walls, and the boundary conditions prescribed at flow inlets and outlets are listed in Tbl. 1. A small high pressure, high temperature kernel was used at the start of the simulation to ignite the reactants. The ignition kernel initiated detonation waves within the annulus, which eventually gave way to periodic behavior. In all, the mesh consisted of 99M cells, and it took 5.7M cpu hours to simulate the first 2ms of physical time using the Onyx high performance computer, part of the DoD Supercomputing Resource Center.

3 Idealized Laser Absorption Measurements

The end result of a laser absorption diagnostic is a measurement of flow properties based on the region of gas that interacts with the laser. One targeted measurement is of the amount of species that is encoun-

tered – a molar density, e.g., moles per meter^3, representative of a path-integration of the moles of the targeted species present in the gas. The average molar density $\bar{n_j}$ of species j taken with a laser path of length L then depends on the local molar density n_j by a direct integral relation:

$$\bar{n}_j L = N_j = \int_0^L n_j \, dl \tag{1}$$

Similarly, experimental measurements of temperature are based on the absorbance characteristics of the species, and so are again based on a species-weighted path-integration. For temperature T, the comparable measurement is an average (denoted $\bar{T}$):

$$\bar{T} = \frac{\int_0^L n_j T \, dl}{N_j} \tag{2}$$

This can be taken advantage of in simulations, since N_j and $\bar{T}$ are both easy to calculate as derived quantities using simulation species and temperature outputs. Modeling a laser according to Eqs. 1 and 2 is a representation of a perfect Beer-Lambert based absorption diagnostic, and does not take into account many significant difficulties that must be considered when designing this sort of diagnostic; however, it allows an evaluation of the difficulties encountered when interpreting a real diagnostic measuring three-dimensional mixing fields present in RDREs.

4 Results and Discussion

Table 2: Summary of global quantities for simulation and experimental results. CTAP1 and CTAP2 measurements are taken 0.009 m and 0.029 m, respectively, from the injection plane. Given simulation wave velocity is a temporal average

	Waves	Wave Speed	CTAP1	CTAP2	Thrust	Isp
Simulation	2	1613 m/s	0.47 MPa	0.34 MPa	433 N	165 s
Experiment	2	1810 m/s	0.38 MPa	0.30 MPa	358 N	139 s

The simulation developed into two co-rotating waves, and can be directly compared to experimental measurements conducted at AFRL. Table 2 displays global measurements that can be used to confirm that the high fidelity simulation correctly captures the experimental case. The simulation did overpredict chamber pressure and thrust, which is common in RDRE simulations; the increased pressure may stem from losses that are not included in the simulation model, such as heat loss to the walls. However, overall these parameters show that the detonation dynamics of the experiment were quite well captured by the simulation, and the same number of waves allows for a direct comparison of the time-varying effects that would be measured by laser diagnostics.

The flowfield upstream of the detonation developed into a complex mixing field, with hot combustion products recirculating near the walls of the chamber. As a consequence, any laser diagnostic based on path measurements inside the field would travel through both a high-temperature product region and the low-temperature reactant region, skewing results away from the quantity of interest. An example of this challenge is shown in Fig. 2, with an overlayed line to indicate a representative laser path. In order to measure a temperature that can be connected to a temperature in of an actual location, the cold and hot temperatures portions of the laser would need to be somehow separated.

Fig. 2 also suggests one possible flow feature that can be used to isolate different portions of the flow: the species present at each location. The cold parts of the flow contain unburnt reactants; consequently,

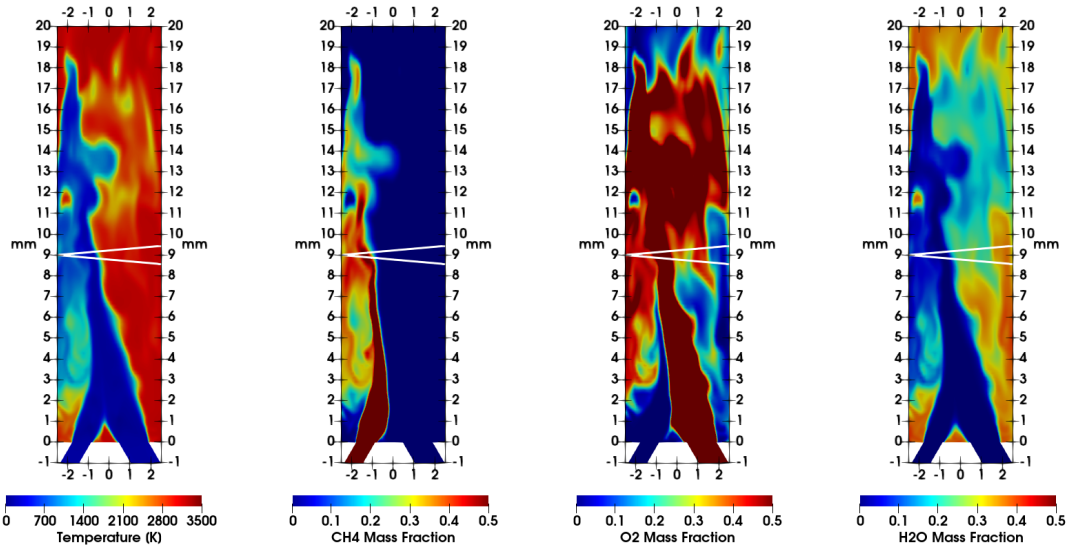

(a) (b) (c) (d)

Figure 2: Flowfield snapshots in front of the detonation structure, with white line indicating a laser path.

this is the region that contains the majority of flow's methane. Similarly, as a final product, water is mostly located in the high temperature region.

What this spatial separation means for an instantaneous laser path is shown in Fig. 3. This figure shows directly that the cold portions of the flow correspond to injected methane and oxygen. Dashed lines in Fig. 3 represent species-weighted temperature measurements, as in Eq. 2; these ideal temperature measurements show that targeting methane yields a temperature average overlapping the cold region, water yields a temperature near the hot region, and because oxygen exists in both the product and reactant regions, an oxygen-weighted temperature would be between the two.

There are still several challenges that appear in the species-weighted temperature measurements of Fig. 3. The first is that the cold core which contains methane is spread over a large range of temperatures, and so although the average of this region would be accurately measured by an ideal methane-weighted measurement, the resultant temperature still does not directly equate to an accurate measurement for a specific point, which is what would be more desirable when measuring detonative properties. Further, the molar density of water is comparatively low throughout the laser path, and because there is some mixing between the two zones a temperature measurement targeting water would still be an underestimate of the recirculation zone temperature.

The evaluation of idealized laser absorbance measurements targeting methane and water is extended in Fig. 4 to consider time-varying effects, with column density evaluated according to Eq. 1, and species-weighted temperature according to Eq. 2. An important aspect of the column density measurements is that the amount of water spikes with the passing of the detonation wave; this is not surprising, but it suggests that product column density can be used to locate passing waves even in the absence of a pressure measurement. Methane largely disappears after the passage of a wave, and cannot be used to evaluate temperature in that region of the flow; however, unlike in the water signal, drops in temperature corresponding to species in the fill region appear in the methane-weighted temperature signal. Combining simultaneous measurements of methane and water provides composition and species information for the entire period, and is a promising approach for temporally-resolved measurements in the detonation region of an RDRE.

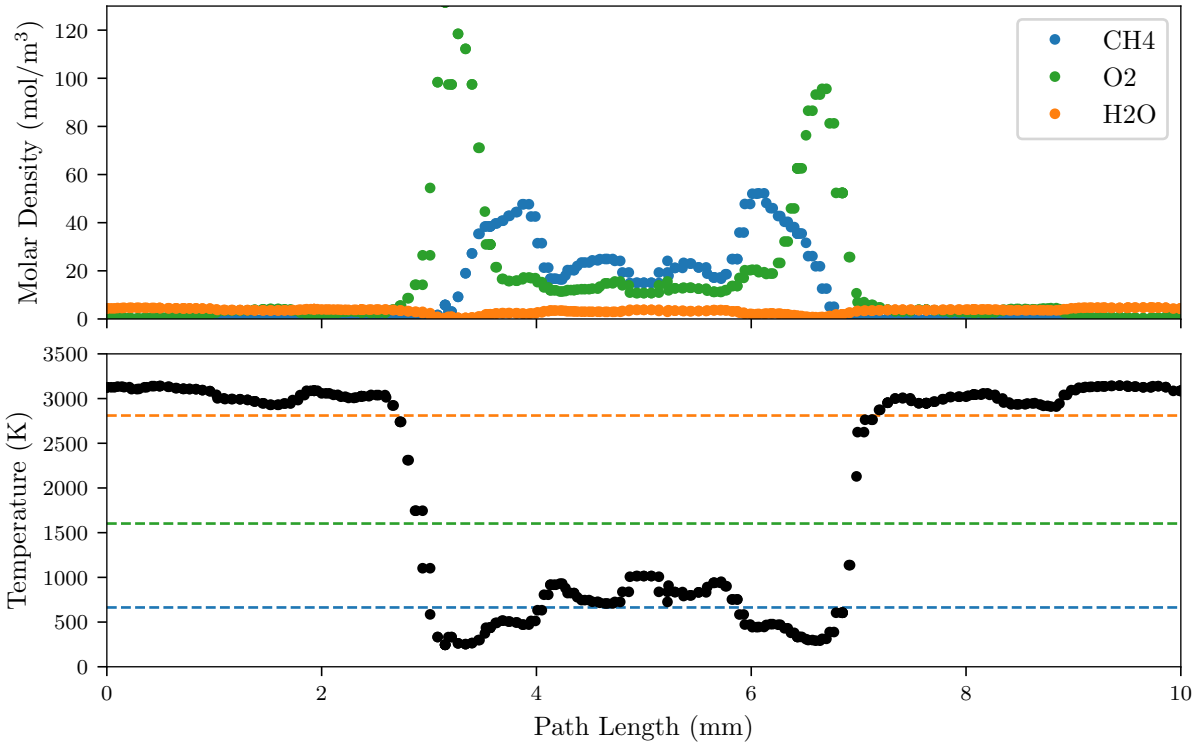

Figure 3: Species molar densities (top) and flow temperature (bottom) at locations along the path shown in Fig. 2. Horizontal lines indicate species-weighted temperature measurements for the full path, as in Eq. 2.

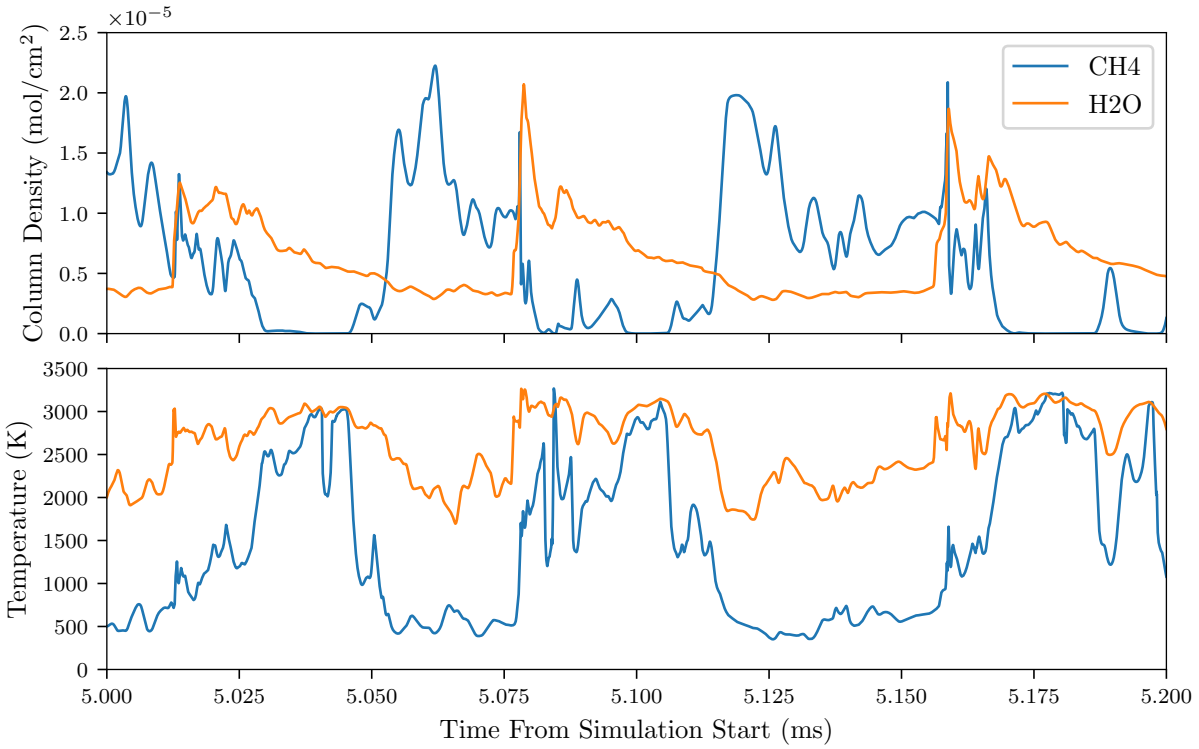

Figure 4: Species-weighted composition (top) and temperature (bottom), for an ideal LAS diagnostic targeting methane and water.

5 Conclusions

Laser measurements of RDRE flowfields must take into account the three-dimensional nature of the relevant mixing fields. A simulation of a gaseous methane-oxygen RDRE was used to consider idealized laser absorption measurements in the vicinity of the detonation. This analysis suggests that targeting methane and water could be used to isolate spatial regions in a way that provides meaningful information about the flowfield. There still remain a number of technical challenges to be overcome before this sort of measurement can be taken experimentally in an RDRE, but this provides a first step towards designing diagnostics capable of evaluating what is truly happening near injection in an RDRE.

6 Acknowledgments

This work has been supported by the Air Force Office of Scientific Research (AFOSR), under AFRL Lab Task 23RQCOR010 funded by the AFOSR Energy, Combustion, and Non-Equilibrium Thermodynamics portfolio with Chiping Li as program manager. Additionally, the work was supported in part by high-performance computer time and resources from the DoD High Performance Computing Modernization Program. The views expressed are those of the authors, and do not necessarily reflect the official policy or position of the Department of the Air Force, the Department of Defense, or the U.S. Government.

References

[1] A. P. Nair, D. D. Lee, D. I. Pineda, J. Kriesel, W. A. Hargus, J. W. Bennewitz, S. A. Danczyk, and R. M. Spearrin, "MHz laser absorption spectroscopy via diplexed RF modulation for pressure, temperature, and species in rotating detonation rocket flows," *Applied Physics B*, vol. 126, no. 8, p. 138, Aug. 2020.

[2] A. P. Nair, D. D. Lee, D. I. Pineda, J. Kriesel, W. A. Hargus, J. W. Bennewitz, B. Bigler, S. A. Danczyk, and R. M. Spearrin, "Methane-oxygen rotating detonation exhaust thermodynamics with variable mixing, equivalence ratio, and mass flux," *Aerospace Science and Technology*, vol. 113, p. 106683, Jun. 2021.

[3] W.-W. Kim and S. Menon, "An unsteady incompressible Navier–Stokes solver for large eddy simulation of turbulent flows," *International Journal for Numerical Methods in Fluids*, vol. 31, no. 6, pp. 983–1017, 1999.

[4] M. Masquelet and S. Menon, "Large-Eddy Simulation of Flame-Turbulence Interactions in a Shear Coaxial Injector," *Journal of Propulsion and Power*, vol. 26, no. 5, pp. 924–935, Sep. 2010.

[5] G. P. Smith, Y. Tao, and H. Wang, "Foundational Fuel Chemistry Model Version 1.0 (FFCM-1)," 2016.

[6] S. Badillo-Rios, "Effect of Chemical Kinetic Mechanisms on Turbulent Combustion," Ph.D. dissertation, UCLA, 2020.